RSC Advances

PAPER

View Article Online
View Journal | View Issue

Cite this: *RSC Adv.*, 2021, **11**, 35946

Fluorescent "on–off–on" sensor based on N,S co-doped carbon dots from seaweed (*Sargassum carpophyllum*) for specific detection of Cr(VI) and ascorbic acid†

Hua Tian,‡ Guangxu Ju, Mengting Li, Wenzhe Fu, Yongcheng Dai, Zhenyi Liang, Yuheng Qiu, Ziyu Qin* and Xueqiong Yin *

A low-temperature carbonization method using seaweed (*Sargassum carpophyllum*) as a precursor was applied to prepare nitrogen and sulfur co-doped CDs (N,S-CDs). The N,S-CDs exhibited satisfactory stability, water solubility and photostability. The N,S-CDs-based "on–off" fluorescent sensor showed high selectivity and good response to Cr(VI), whose limit of detection (LOD) was as low as 1.04 μM. The recoveries of Cr(VI) in tap water and sea water were 88.90–116.38% (RSD < 5%), proving that it could be a practical sensor for detecting Cr(VI). In addition, the established N,S-CDs/Cr(VI) system was developed as an "off–on" fluorescent sensor to detect ascorbic acid (AA). It could precisely detect AA in vitamin C chewable tablets, with recoveries from 96.02 to 103.95% (RSD < 5%). Moreover, the N,S-CDs expressed low toxicity by CCK8 assay. In this work, an "on–off–on" fluorescent sensor was prepared from seaweed, which can act as a reference for enabled high-value transformation of seaweeds. Furthermore, it also provided a facile fluorescent sensor for the detection of Cr(VI) and AA. The fluorescent sensor expressed high potential in water quality monitoring and nutritional food quality control.

Received 31st August 2021
Accepted 22nd October 2021

DOI: 10.1039/d1ra06544k

rsc.li/rsc-advances

Introduction

With the progress of society and the continuous improvement of living standards, people express higher requirements for their health, and pay more attention to food quality and nutrition in their diet. However, in recent decades, environmental pollution has caused serious risks to the food supply, such as heavy-metal ion and organic compound contamination, nutrient deficiency, *etc.* It is necessary to detect harmful ingredients and nutrients in food. Chromium is a hazardous heavy-metal ion and exists primarily as trivalent chromium (Cr(III)) as well as hexavalent chromium (Cr(VI)).[1,2] Cr(VI) is regarded as harmful to human beings because it cannot be biodegraded, and is easily enriched in organisms and then accumulated in the human body through the food chain. For example, chromium content in different marine fishes from the coastline of Hainan (South China Sea) ranged from 1.38 to 4.36 mg kg^{-1},[3] exceeding the maximum limit for aquatic animals allowed by the National Food Safety Standard of China (GB, 2762-2012). To measure the concentration of Cr(VI), many methods including inductive electrochemical methods, atomic absorption spectrometry, coupled plasma mass spectrometry, *etc.*, have been used.[4–6] Nevertheless, these methods have some disadvantages, such as requiring expensive equipment and tedious sample pretreatment, limiting their application in rapid detection. Thus, it's urgent to quantify the Cr(VI) concentration rapidly in water and food to avoid excessive intake of Cr(VI). Furthermore, ascorbic acid (AA) as a kind of important nutrient in food also needs a proper detection method. AA is a water-soluble vitamin exists widely in health-oriented products, vegetables and fruits. It is indispensable in the formation of carnitine, neurotransmitters and collagen.[6] Besides, as a strong antioxidant, AA can eliminate free radicals in metabolism and prevent humans from causing many diseases, such as angiocardiopathy, parkinsonism, cancer, and so on.[7] The Food and Nutrition Board of National Academies recommends the average amount of AA for male and female a day is 90 mg and 75 mg respectively, and the maximum daily intake for an adult is about 2000 mg.[8] So the detection of AA is also very important. There are numerous detection methods for AA, such as colorimetry,[9] electrochemistry,[10] chromatography,[11] photoluminescence,[12] chemiluminescence,[13] fluorescence (FL) spectroscopy,[14] and so on. Among them, the application of FL spectroscopy is more widely owing to its simplicity, rapid response, low cost, and high sensitivity.

In recent years, carbon dots (CDs) have received great attention because they have many outstanding benefits including water solubility, small size, excellent photostability,

Hainan Provincial Fine Chemical Engineering Research Center, Hainan University, Haikou, Hainan, 570228, P. R. China. E-mail: ziyuqin@hainanu.edu.cn; yxq88@hotmail.com

† Electronic supplementary information (ESI) available. See DOI: 10.1039/d1ra06544k

‡ Authors contributed equally to the work.

tunable excitation/emission, favorable biocompatibility and lower cytotoxicity.[15] CDs are excellent promising fluorescent nanomaterials. At present, the preparation of fluorescent CDs has two synthetic paths, namely top-down and bottom-up. The synthesis of CDs by decomposing large carbon structures into small clusters are considered the top-down methods, which involve arc laser ablation, electrochemical oxidation, electric discharge, *etc.*[16] However, such methods are limited by the specific instruments and expensive raw materials. Low-temperature carbonization, microwave heating, combustion/heat treatment and hydrothermal treatment are considered bottom-up methods, which are simple and green. In the bottom-up approaches, CDs are formed in a controlled manner by different small/big molecule precursors such as carbohydrates, organic acid, natural resources.[17] Natural resources (such as fruit,[18] olive leaves,[19] flowers[20]) are cost-effective, environmentally-friendly and widely available for the preparation of CDs.[21] Moreover, the multiple components (protein, amino acid, carbohydrates and vitamin, *etc.*) in natural resources could influence functional groups (carboxylic, amino, and hydroxyl groups) of CDs and improve the optical performances, eventually enhance the sensitivity and selectivity for target molecules.[22]

Recently, natural sources are developed to prepare nitrogen and sulfur co-doped CDs (N,S-CDs) due to their superior performance, which can be applied in chemical sensing, biosensing, and nanomedicine.[23] N,S-CDs are generally synthesized by using nitrogenous and sulphureous chemical reagents for the surface passivation and functionalization of CDs. However, these chemical reagents can cause some drawbacks, such as potential hazard and time-consumption.[24] Seaweeds are abundant natural resources, there are over 30 000 kinds of seaweeds in the worldwide ocean, which have many chemical ingredients, including cellulose, amino acids, polysaccharides, fatty acid and vitamins.[25] Therefore, seaweeds could be chosen as a good natural carbon source for nitrogen and sulfur co-doped CDs (N,S-CDs) preparation. Traditionally, seaweeds are utilized as food or health care products, and the commercial utilization of seaweeds are used as sources of agar production and aquaculture feeds.[26] Seaweeds have the advantages of low cost, abundant resources, high carbon content. However, the complex separation of algal components and the single utilization mode limit the high-value transformation and utilization, resulting in resource waste and environmental pollution. In order to solve these problems, seaweeds have been explored for health care product, skin care product, and other functional materials. To our best knowledge, there is no report about the preparation of CDs from seaweeds. If seaweeds can be proved to prepare functional CDs successfully, this will provide abundant raw material options for the preparation of CDs and a reference for enabled high-value transformation of seaweeds. *Sargassum carpophyllum* is one of brown seaweed species widely distributed in the temperate and tropical oceans, especially in the South China Sea, which is an easily available precursor for CDs preparation in Hainan.

Herein, N,S-CDs were synthesized through a low-temperature carbonization treatment of *Sargassum carpophyllum*. The prepared N,S-CDs-based fluorescent sensor could be directly used to detect Cr(VI), then AA would regain the quenched FL of N,S-CDs by Cr(VI). According to these phenomena, an "on–off–on" fluorescent sensor for detecting Cr(VI) and AA was designed (Scheme 1). The experimental results show that the detection mechanism of Cr(VI) and AA is due to the internal filtering effect (IFE) of N,S-CDs, which is conducive to the quenching of its FL by Cr(VI). While AA can reduce Cr(VI), leading to the IFE decreasing and the FL of N,S-CDs recovering. In addition, the established fluorescent sensor was applied to real samples with satisfactory results. Furthermore, the low toxicity of N,S-CDs was tested by CCK8 assay.

Materials and methods

Materials

The raw material of *Sargassum carpophyllum* was picked from Nanyanwan Beach in Wanning City, Hainan Province, China. $BaCl_2 \cdot 2H_2O$, $CaCl_2$, $CdN_2O_6 \cdot 4H_2O$, $Cr(NO_3)_3 \cdot 9H_2O$, $Cu(NO_3)_2 \cdot 4H_2O$, $K_2Cr_2O_7$, $FeSO_4 \cdot 7H_2O$, $FeCl_3$, $HgCl_2$, $Mg(NO_3)_2 \cdot 6H_2O$, $Pb(NO_3)_2$, KF, KI, KBr, Na_2S, $NaBH_4$, $K_2S_2O_3$, Na_2SO_3 were purchased from Guangzhou Chemical Reagent Factory (Guangzhou, China). Ascorbic acid (AA), glucose, glutathione (GSH), cysteine (Cys) and citric acid were provided by Solarbio Science & Technology Co., Ltd. (Beijing, China). Procell Life Science & Technology Co., Ltd provided the L929 cells. Fetal bovine serum (FBS) was purchased from BI (Biological Industries, Israel). Dulbecco's Phosphate Buffered Saline (D-PBS) buffer was obtained from GenvieW (GenvieW, US). Dulbecco's modified Eagle's medium (DMEM) was supplied by Gibco (Thermo Fisher Scientific, US). Vitamins C chewable tablets were obtained from Zhejiang CONBA Health Technology Co., Ltd. Cell Counting Kit-8 (CCK-8) was supplied by Dojindo Chemical Laboratories (Kumamoto, Japan).

Characterization

The transmission electron microscopy (TEM) and the high resolution transmission electron microscopy (HRTEM) images

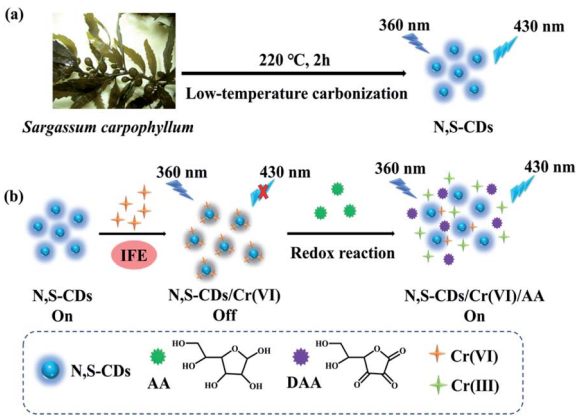

Scheme 1 Synthetic route of N,S-CDs from *Sargassum carpophyllum* (a) and detection mechanism of Cr(VI) and AA (b).

were observed on a JEM-2100 microscope under acceleration voltage of 200 kV. The PHI5000 Versaprobe-II spectrometer with a monochromatic AI Kα (1486.6 eV) source was applied to collect X-ray photoelectron spectroscopy (XPS) data. The result of Fourier transform infrared (FTIR) spectroscopy was obtained on a TENSOR27 spectrometer (Bruker, Germany) by using KBr pellets. The crystallinity was measured by a X-ray diffraction (XRD) instrument (Bruker D8) using Cu-Kα radiation ($\lambda = 1.541$ Å) in the 2θ ranging from 10° to 80°. The UV-vis absorption spectra were obtained using a TU-1901 UV-vis spectrophotometer (China). The FL life time was measured on an FLS 920 fluorescence spectrophotometer (Edinburgh Instruments Ltd., U K). FL emission spectra were recorded by a F-320 fluorescence spectrophotometer (China).

Preparation of N,S-CDs

Sargassum carpophyllum was washed with water, air-dried and cut into thin slices for further processing. 5.0 g *Sargassum* fragments were placed in the crucible and carbonized in a muff furnace. Different carbonization time (0.5–3 h) and temperature (160–260 °C) were varied for optimization purposes. After cooling, the carbonized product was obtained for further processing. The obtained mixture was dispersed in ultrapure water, then sonicated for 30 min, and centrifuged at 10 000 rpm for 10 min to separate the precipitate. The supernatant was filtrated with 0.22 μm filter membrane and the final filtrate was dialyzed 48 h in a dialysis tube with a molecular weight cut-off 500–1000 Da. Ultimately, the purified N,S-CDs solution (10 mg mL^{-1}) was stored at 4 °C for subsequent experiments.

Quantum yield

The quantum yield (QY) was determined depending on a definite reference, using quinine sulphate (QS) as the control compound. In brief, QS was dissolved in 0.1 M H_2SO_4. The UV-vis absorption of FL emission spectra of QS and sample were measured at 360 nm. The QY of QS was 0.54 at the excitation wavelength of 360 nm.[27] UV-vis absorbance should be kept at about 0.05 to avoid self-absorption effects. The QY of N,S-CDs was calculated by eqn (1).

$$QY = QY_R \times \frac{I_S}{I_R} \times \frac{A_R}{A_S} \times \frac{{n_S}^2}{{n_R}^2} \quad (1)$$

wherein, QY represents the quantum yield; I means the fluorescence peak area; n refers to the solvent refraction index ($n_S/n_R = 1$); and A is the UV-vis absorbance. The subscripts R and S correspond to control and sample, respectively.

Fluorescence detection of Cr(VI)

For the FL detection of Cr(VI), the solution of Cr(VI) was prepared with $K_2Cr_2O_7$. 0.3 mL of 5 mg mL^{-1} N,S-CDs solution and 2.7 mL of 100 μM Cr(VI) solution were added to the cuvette and incubated for 5 min. The FL emission spectra of the mixture solution was measured by FL spectrometer under the excitation of 360 nm. Moreover, the selectivity of the N,S-CDs-based fluorescence sensor and its response to different concentrations of Cr(VI) were also studied.

Fluorescence detection of AA

1 mL of 1 mM Cr(VI) was added into 0.3 mL of 5 mg mL^{-1} N,S-CDs solution to form a sensing platform (N,S-CDs/Cr(VI)). After incubation for 5 min, the FL intensity was monitored by adding 2.7 mL of AA solution (1 mM) at 430 nm under excitation at 360 nm. By adding some reducing agents (KI, KBr, KF, Na_2S, $K_2S_2O_3$, Na_2SO_3, $NaBH_4$, GSH, Cys, citric acid, glucose) instead of AA, the fluorescence was also detected to determine the selectivity of N,S-CDs/Cr(VI) to AA. In addition, various concentrations of AA solution were added to N,S-CDs/Cr(VI), and measured with same procedure.

Cytotoxicity assay

CCK-8 analysis was carried out to evaluate the cytotoxicity of CD *in vitro*.[28] Briefly, L929 cells with an average density of 3.0×10^5 cells per mL were seeded in a 96-well microplate with complete medium. After 24 h of incubation (37 °C, 5% CO_2), the fresh DMEM mediums containing serial concentrations of N,S-CDs (0–1000 μg mL^{-1}) were added into the plate well. After a further day of incubation, 10 μL of CCK-8 solution was dropped into each well and incubated for 2 hours. Cells treated with pure medium were the control group. Finally, the absorbance of each well at 450 nm was determined by an ELISA plate reader. The cell survival rates were calculated according to eqn (2).

$$\text{Cell viability } (\%) = \frac{A_S - A_0}{A_C - A_0} \times 100\% \quad (2)$$

where, A_s, A_c, A_0 is the absorbance of the sample, control and blank medium, respectively.

Sample analysis under actual conditions

Sea water was obtained from Meilisha Beach of the South Sea, Haikou, Hainan, China. Local tap water and sea water were collected, centrifuged at 10 000 rpm for 20 minutes, and filtered with a 0.45 μm membrane filter to remove impurities. After the pretreatments, 2.7 mL samples and 0.3 mL of 5 mg mL^{-1} N,S-CDs solution were mixed to detect the Cr(VI) concentration. Then, different concentrations of Cr(VI) standard solutions were added to the N,S-CDs solution by the standard addition method.[29] The FL intensity was measured under the excitation of 360 nm.

Two vitamins C chewable tablets were ground into powders with a mortar. Subsequently, 2.4172 g of powder was dispersed with 50 mL ultrapure water and treated with ultrasonic for 10 min. The suspension was further centrifuged at 8000 rpm for 10 min to remove the precipitation. Then, the supernatant was filtered through a 0.45 μm Millipore filter. Finally, 1 mL of the solution was diluted 100 times with ultrapure water for analysis. The detection method of AA in vitamins C chewable tablets was consistent with that of fluorescence detection of AA.

Results and discussion

Synthesis of N,S-CDs

The N,S-CDs were prepared by treating *Sargassum carpophyllum* using the low-temperature carbonization method (160–260 °C)

in a muffle furnace under ambient pressure condition. The two effect factors (carbonization time and temperature) on the QY of the N,S-CDs were optimized. As shown in Fig. S1a,† under the temperatures of 160 °C, 180 °C, 200 °C, 220 °C, 240 °C, 260 °C, the QY were 2.15%, 2.20%, 2.76%, 4.37%, 3.14%, 3.76%, respectively. Fig. S1b† showed that the QY under the carbonization time of 0.5 h, 1 h, 1.5 h, 2 h, 2.5 h, 3 h were 3.58%, 3.35%, 3.84%, 4.37%, 3.86%, 3.91%, respectively. In conclusion, the highest QY 4.37% was achieved at the optimal conditions of 220 °C and 2 h, which is general for the unmodified CDs.[8] As the result shows that the maximum change rate of QY caused by temperature and time was 103.26% and 30.45%, respectively. Therefore, the temperature had greater effect on QY than time. Temperature plays a predominant role in the carbonization process. The carbonization degree increases with increasing temperature, resulting in the transformation of CDs from the surface/molecular state to the carbon core state.[30] Thus, the QY would be changed according to the fluorescent origins. The low carbonization temperature makes the carbonization incomplete, so that the surface/molecular state is the main fluorescent origin. At high temperature, the surface/molecular state is changed to carbon core state due to the further carbonization. At 220 °C, the partial carbon core state is formed and an oxygen-containing functional group appears on the surface of the CD under ambient pressure condition. The FL is induced by the carbon core state and surface/molecular state. Herein, the surface functional group may be reach to equilibrium after reacting at 220 °C for 2 h, so the QY is highest. Compared with other natural resources from which the CDs were synthesized by H_2SO_4/H_3PO_4,[31,32] the method we adopted in this work is greener and simpler.

Characterization of N,S-CDs

Morphology and surface study. The TEM image and the size distribution (inset) of N,S-CDs were shown in Fig. 1a. It can be seen that the N,S-CDs were uniformly dispersed without apparent aggregation and showed spherical shapes. The size distribution graph was performed using Nano Measurer software by taking measurements of 100 counts of the particles. The particle size distribution of N,S-CDs was 0.77–4.62 nm, and the value of the average size was 2.19 ± 0.68 nm. The HRTEM image was given in Fig. 1b. The spacing of lattice fringes was 0.18 nm that was associated with the (102) facet of graphitic carbon, which was indicative of the graphitic nature of the N,S-CDs.[33] The FTIR spectrum of N,S-CDs was shown in Fig. 1c. The wide absorption band appeared at 3420 cm^{-1}, which were assigned to the stretching vibrations of O–H and N–H, and the low intensity peak around 2930 cm^{-1} was related to the stretching vibrations of C–H.[34] The absorption bands at 2343 cm^{-1} and 1680 cm^{-1} were observed, which were due to the presence of C–N and C=O bonds, respectively.[35] The stretching vibration of C=C located at 1583 cm^{-1}.[29] The C–H and N–H stretching vibrations appeared around 1425 cm^{-1}. Meanwhile, the bending vibrations of C–O, C–N and C–S appeared at 1128 cm^{-1}. The bands around 1029 cm^{-1} were corresponded to the presence of C=S, C–O–C, and C–O groups.[35,36] The results

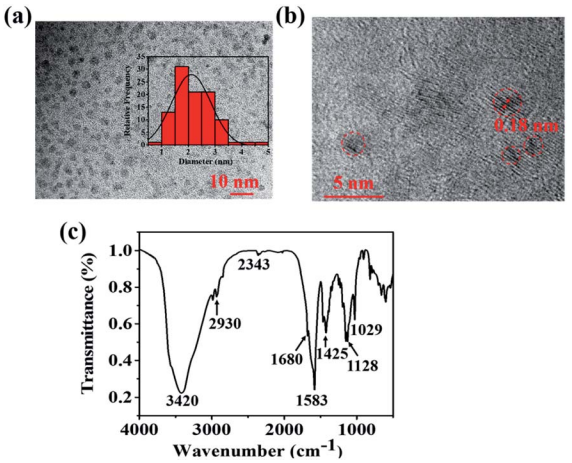

Fig. 1 (a) TEM image (inset: the diameter distribution of N,S-CDs). (b) HRTEM image and (c) FTIR spectrum of N,S-CDs.

indicated that the N,S-CDs contained C=C, C–O, O–H, –COOH, C–N, and C–S groups. All the oxygen-containing functional groups on the surface of N,S-CDs play important roles in increasing the hydrophilicity and stability, which provided great potential for the sensing of N,S-CDs in aqueous samples.[37] As seen from Fig. S2,† the XRD patterns of the N,S-CDs prepared at different temperatures (160–260 °C) appeared at 29.3°. It was consistent with the 002 plane of graphite.[38] And the intensity of diffraction peaks increased with the temperature rising. It indicated the higher temperature caused a higher carbonization degree.

As shown in Fig. S3,† the XPS resulted of N,S-CDs showed four typical peaks of S2p (168.2 eV), C1s (284.2 eV), N1s (400.2 eV) and O1s (531.2 eV), which showed that C : N : O : S was 72.07%, 1.13%, 25.55%, 1.26%. Other obvious peaks at 305.2 eV and 497.2 eV were assigned to K (loss) and Na (Auger), which was resulted from the absorption effect of K and Na ions.[39] Fig. 2 displayed the high-resolution XPS spectra. The peaks (Fig. 2a) at 168.5, 169.3, 169.9 eV were related to –C–SO_x (x = 2, 3, 4), respectively.[34] This may be attributed to the fucoidan in brown seaweed, which contains sulphates. The peaks (Fig. 2b) at 282.0,

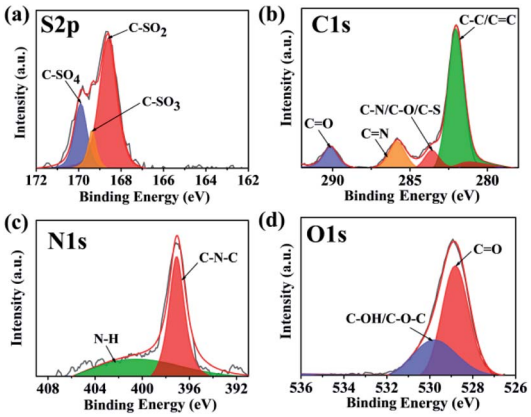

Fig. 2 XPS spectra of the N,S-CDs ((a) S2p, (b) C1s, (c) N1s and (d) O1s).

283.6, 285.8, 290.1 eV represented the existence of C–C or C=C, C–N or C–O or C–S, C=N or C=O.[40] In the high-resolution spectrum of N1s, the two peaks at 397.0, 401.2 eV (Fig. 2c) are attributed to the C–N–C, N–H groups, respectively.[41] Besides, the peaks of O1s (Fig. 2d) at 528.8, 529.8 eV referred to the form of C=O, C–O or C–O–C bonds, respectively. The XPS results were in accord well with the FTIR analysis, which indicated the N,S-CDs were composed of multiple functional groups. The zeta potential of CDs is -11.73 ± 0.85 mV. Due to the existence of chemicals in brown seaweeds, such as fatty acid, vitamins, amino acids, fucoidan, the prepared N,S-CDs contain carboxyl groups, amino groups, and sulfate groups, *et al.* Comparing to CDs from other natural resources (such as mango and *Prunus cerasifera*),[18,31] the N,S-CDs from *Sargassum carpophyllum* contain more functional groups, such as sulfate groups. These functional groups make CDs have good water solubility and excellent optical properties.[7]

Optical properties

To verify optical properties of N,S-CDs, the UV-vis and FL spectroscopy were studied. Fig. S4a† revealed that the UV-vis spectra of the N,S-CDs showed a strong absorption peak around 270 nm because of the transition of π–π* for the C=C bond.[42] When the N,S-CDs were excited with the excitation wavelength at 360 nm, they exhibited strong blue FL around 430 nm. In addition, the FL properties of N,S-CDs at different excitation wavelengths were studied. Fig. S4b† described that when the excitation wavelength red-shifted from 330 to 380 nm, the emission peaks changed from 425 to 435 nm. The results showed the FL intensity first increased and then decreased, and the maximum FL intensity of the emission peak appeared at 430 nm. The optimal excitation wavelength referred to 360 nm and the emission wavelength was at 430 nm. Herein, the emission wavelength shifted towards longer wavelengths (red shift) while increasing the excitation wavelength. It indicated that the N,S-CDs possessed excitation-wavelength-dependent photoluminescence behaviour, which could be due to the surface states and different sizes.[43]

Furthermore, Fig. S5a and S5b† showed the photostability of N,S-CDs. The N,S-CDs still expressed strong FL after irradiation by 365 nm UV light for 60 min and keeping for 30 days at room light. It showed that the N,S-CDs had excellent anti-photobleaching property and FL stability. In addition, Fig. S5c† indicated that the FL intensity had no significant change under various NaCl concentrations (0–1.0 M). The result revealed that N,S-CDs was stable in the salty environment. In Fig. S5d,† pH (3.0–12.0) had almost no effect on the FL intensity. Therefore, the influences of ionic strength and pH value of the solution on the FL stability of N,S-CDs were negligible. These results revealed the N,S-CDs had good stability and antijamming capability, and could be used for sensing applications in real environment.

Detection of Cr(VI)

The quenching ability of various ions to the N,S-CDs was examined. As shown in Fig. 3a and b, Cr(VI) exhibited the most noticeable FL quenching effect on N,S-CDs, whereas the equal amount of possible interfering metal ions (Cd^{2+}, Ca^{2+}, Mg^{2+}, Cr^{3+}, Ba^{2+}, Fe^{2+}, Cu^{2+}, Fe^{3+}, Hg^{2+}, and Pb^{2+}) and anions (Cl^-, CO_3^{2-}, HPO_4^{2-}, SO_3^{2-}, ClO^-, $H_2PO_4^-$, SO_4^{2-}) showed no obvious quenching effect[44,45] (black bars). Therefore, it could be considered that other metal ions had little effect. In addition, the selectivity and anti-interference ability of the N,S-CDs in testing Cr(VI) was also evaluated. Cr(VI) was mixed with the N,S-CDs solution containing another metal ions and anions. Comparing the system with (red bars) or without Cr(VI) (black bars), the relative fluorescence intensities (F/F_0) decreased markedly when Cr(VI) was present. The consequences revealed the high selectivity of N,S-CDs for detecting Cr(VI).

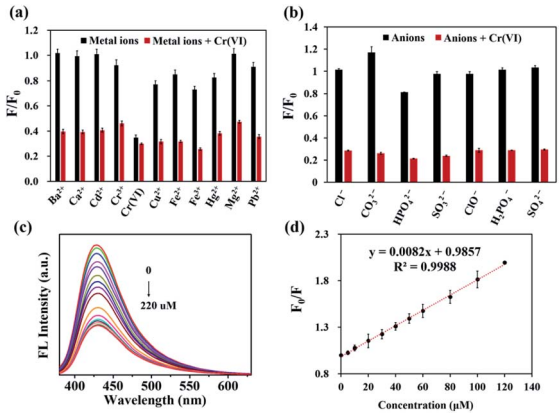

Fig. 3 Fluorescence-quenching efficiency and interference effects of various metal ions (a) and anions (b), where F_0 and F are the fluorescence intensity of N,S-CDs (5 mg mL^{-1}) in the nonexistence and existence of various interfering ions (Cr(VI), metal ions and anions: 100 μM). (c) FL spectra of N,S-CDs in the presence of different concentrations of Cr(VI) (0–220 μM). (d) F_0/F *versus* Cr(VI) concentration in the range from 0 to 120 μM, where F_0 and F are the FL intensity of the N,S-CDs in the absence and presence of Cr(VI) ($\lambda_{ex} = 360$ nm; $\lambda_{em} = 430$ nm).

The analytical performance of N,S-CDs for Cr(VI) measurement was investigated to verify its feasibility. The FL spectra of N,S-CDs in Cr(VI) solutions with different concentration (0–220 μM) were recorded. Fig. 3c showed that the FL intensity of N,S-CDs decreased with increasing the concentration of Cr(VI). Fig. 3d displayed that there was a good linear relationship between F_0/F and the concentration of N,S-CDs in the range from 0 to 120 μM. And the linear regression equation was $F_0/F = 0.0082\ [Cr(VI)]\ \mu M + 0.9857$ ($R^2 = 0.9988$). The limit of detection (LOD) of Cr(VI) was estimated to be 1.04 μM according to the formula ($LOD = 3\sigma/S$, wherein σ is the standard deviation of the blank signals, S represents the slope of the linear curve).[46] Compared with the previous reported literatures presented in Table S1,† the N,S-CDs in this work expressed better detection performance for Cr(VI). Based on the excellent performance, the N,S-CDs as a "turn-off" fluorescent sensor own unique superiorities of sensitivity, selectivity, convenience, green preparation, stability, fast response, origin from renewable resources, *etc.* Thus, it is promising to develop its potential application for detecting Cr(VI) in water from real environments.

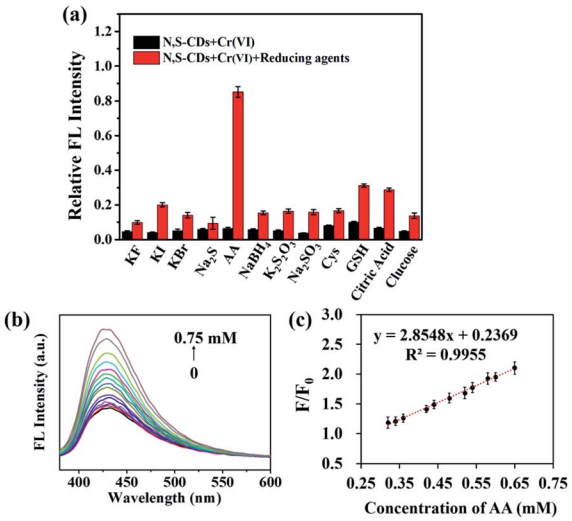

Fig. 4 (a) FL intensity of N,S-CDs/Cr(VI) system after the addition of different reductants (reductant 1 mM; Cr(VI) 1 mM). (b) FL responses of N,S-CDs/Cr(VI) system upon addition of various concentrations of AA (0–0.75 mM). (c) Linear relationship between F/F_0 and AA concentration in the range of 0.32–0.65 mM (F and F_0 represent the FL intensities of 430 nm in the presence and absence of AA, respectively) (λ_{ex} = 360 nm; λ_{em} = 430 nm).

Detection of AA

The as-prepared N,S-CDs/Cr(VI) was employed to detect AA based on the redox reaction between Cr(VI) and AA. Fig. 3a revealed that Cr(III) did not caused significant changes in the FL intensity of N,S-CDs. Here, the effects of different reductants (including KF, KI, KBr, Na_2S, AA, $NaBH_4$, $K_2S_2O_3$, Na_2SO_3, Cys, GSH, citric acid, and glucose) on the FL recovery of N,S-CDs were researched. As shown in Fig. 4a, among the above reductants, only AA can recover the FL of N,S-CDs/Cr(VI). This result indicated that the fluorescent sensor was specific to AA. Therefore, the quenching FL of the N,S-CDs/Cr(VI) could be restored by AA. It may be that the functional groups in AA could

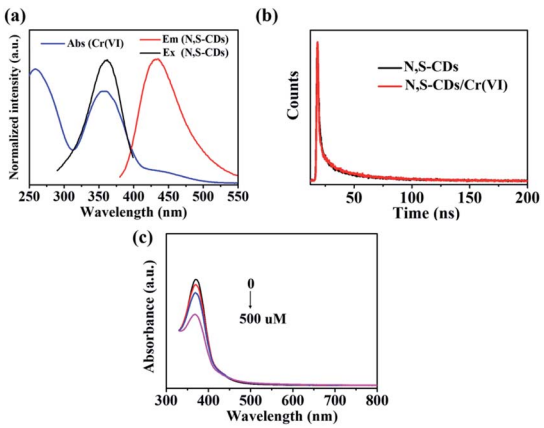

Fig. 5 (a) The UV-Vis absorption spectra of Cr(VI), FL excitation spectra and emission spectra of N,S-CDs in aqueous solution. (b) FL lifetime of CDs in the absence and presence of Cr(VI). (c) UV-vis absorption spectra of N,S-CDs/Cr(VI) system in the presence of different concentrations of AA (λ_{ex} = 360 nm; λ_{em} = 430 nm).

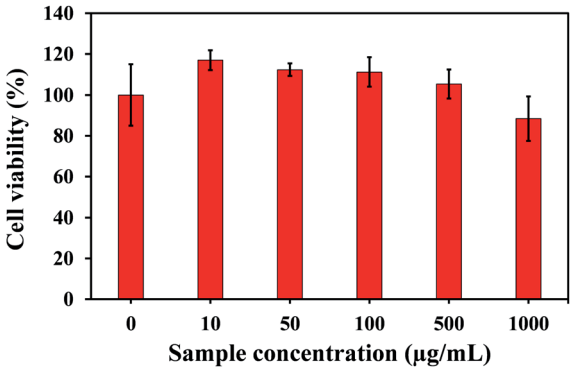

Fig. 6 Viability of L929 cells after incubating with a series of N,S-CDs at 37 °C for 24 h.

eliminate the chelation effect between N,S-CDs and Cr(VI), and then reduce the Cr(VI) to Cr(III).[6] From Fig. 4b, it showed that the FL intensity of the N,S-CDs/Cr(VI) system gradually enhanced while the concentration of added AA increased. In Fig. 4c, there was a good linear relationship between the FL recovering efficiency and the concentration of AA. The linear correlation equation was as follows: F/F_0 = 2.8548 [AA] mM + 0.2369 (R^2 = 0.9955) in the range of 0.32–0.65 mM. The theoretical LOD was 2.99 μM in terms of the formula LOD = $3\sigma/S$. The results expressed that N,S-CDs/Cr(VI) had the chance to be applied as an "off–on" FL sensor for detecting AA in vitamin C-rich health products and medicines.

Further comparison with the previous reported methods presented in Table S2,† it implied that our sensor possessed abundant natural raw materials, green and simple preparation method, as well as the comparable linear range and detection limit. The natural resource seaweeds used as a kind of carbon resource is a sustainable process as a paradigm of reclamation of wastes and it will ease the problem of waste accumulation and provide an economical way compared with the use of industrial chemicals.[47]

Mechanism study of Cr(VI) and AA detection strategy

By comparing the UV-vis absorbance spectrum of Cr(VI) with the FL excitation spectrum and emission spectrum of N,S-CDs, the FL quenching mechanism of N,S-CDs by Cr(VI) were discussed. As illustrated in Fig. 5a, the UV-vis absorption peaks at 258 nm,

Table 1 Cr(VI) detection in sea water and tap water samples[a]

Samples	Initial amount (μM)	Added (μM)	Total detected (μM)	Recovery (%)	RSD (%)
Sea water	15.04	50	62.07	88.91	2.99
		75	102.33	116.38	1.68
		100	115.15	100.11	4.68
Tap water	ND	50	45.09	90.18	2.85
		75	80.43	107.24	4.46
		100	91.76	91.76	1.24

[a] RSD – relative standard deviation of three replicates, ND – not detected.

Table 2 AA determination in vitamins C chewable tablets[a]

Sample	Initial amount (mg g^{-1})	Initial amount (μM)	Added (μM)	Total detected (μM)	Recovery (%)	RSD (%)
Vitamins C chewable tablets	169.20	464.34	50	512.35	96.02	3.30
			100	568.29	103.95	1.68
			150	610.98	97.76	4.08

[a] RSD – relative standard deviation of three replicates.

357 nm, and 430 nm attributed to Cr(VI). The N,S-CDs had an excitation peak around 360 nm and an emission peak located at 430 nm, respectively. It indicated that the absorption spectrum of Cr(VI) not only overlapped precisely with the excitation spectrum but also the emission spectrum of N,S-CDs, which could cause part of the emission light from CDs to be shielded by Cr(VI) because some excitation energy of the CDs was subdued.[48,49] What's more, the lifetimes of N,S-CDs and N,S-CDs/Cr(VI) were presented in Fig. 5b. The average lifetime values of N,S-CDs and N,S-CDs/Cr(VI) are analyzed to be 1.11 ns and 1.18 ns, respectively. The FL lifetimes had almost no change, presenting a static quenching effect. It indicated the FL quenching mechanism of N,S-CDs towards Cr(VI) was referred to the inner filter effect (IFE), which occurred between the fluorophore and absorber due to the absorption of the emission and/or excitation light of the fluorophore by the absorbers in detection system.[50,51] In addition, the UV-vis absorbance spectrum of N,S-CDs/Cr(VI) at different concentration of AA were recorded to research the mechanism of N,S-CDs/Cr(VI) towards AA. As shown in Fig. 5c, the UV-vis absorption of Cr(VI) (100 μM) at 357 nm visibly decreased when the concentration of AA was 0, 100, 200, 500 μM, respectively. In the presence of AA, the chelation effect between N,S-CDs and Cr(VI) was removed, then Cr(VI) was released and reduced by AA, resulting in the weakening of the IFE, and then caused the FL recovery of N,S-CDs. Based on the above principles, an available "on–off–on" FL sensor for detecting Cr(VI) and AA was established successfully.

CCK8 assay of N,S-CDs

The cytotoxicity of N,S-CDs on L929 cells were tested by CCK8 assay in order to assess the biocompatibility of the N,S-CDs. L929 cells were treated with various concentrations of N,S-CDs in the range of 0–1000 μg mL^{-1}. As illustrated in Fig. 6, the cell viabilities were 117.03 ± 4.81%, 112.40 ± 3.01%, 111.27 ± 7.15%, 105.42 ± 7.13%, 88.46 ± 10.91% when the concentrations of N,S-CDs varied from 10 to 1000 μg mL^{-1}. It indicated the N,S-CDs had no significant effect on cell activity, exhibiting high cell viability.[52] Therefore, the N,S-CDs manifested no cytotoxicity and good biocompatibility. It is beneficial for application in the field of sensing.

Application in real samples

In this work, the sensibility and feasibility of N,S-CDs against Cr(VI) in two water samples (tap water and sea water) were investigated. The recovery assay for different concentrations of Cr(VI) (50, 75, 100 μM) were studied. In Table 1, no Cr(VI) was detected in tap water and the concentration of Cr(VI) in sea water was 15.04 μM. Meanwhile, the recoveries of Cr(VI) in both water samples fall in the commendable ranged (88.90–116.38%) and the relative standard deviation (RSD) was lower than 5%.

Furthermore, the content of AA in the selected brand vitamins C chewable tablet is 177.50 mg g^{-1}, which is commercially available to the public. The application of N,S-CDs/Cr(VI) in detecting AA in vitamins C chewable tablets were shown in Table 2. The content of AA measured by our method in the chewable tablets was 169.20 mg g^{-1}. Compared with the labeled content in the vitamins C chewable tablet, the difference was 4.68%. The recoveries of AA were between 96.02% and 103.95%, with the RSD values lower than 5%. Above results proved the N,S-CDs from seaweed (*Sargassum carpophyllum*) could be a reliable, simple, versatile sensor for detecting Cr(VI) and AA in the real samples.

Conclusions

In conclusion, a new fluorescent N,S-CDs were synthesized from renewable brown seaweed (*Sargassum carpophyllum*) *via* a simple, green and friendly method at first. Then the N,S-CDs were characterized systematically with TEM, FTIR, XPS, UV-vis and fluorescence spectra. The N,S-CDs had nanostructures and abundant functional groups that resulted in good water solubility, excellent photostability and outstanding detection performance. An "on–off–on" FL technique for detecting Cr(VI) and AA has been fabricated using the N,S-CDs as the FL sensor. The "on–off–on" FL sensor displayed good selectivity and high sensitivity to detect Cr(VI) and AA. The FL quenching of N,S-CDs by Cr(VI) was attributed to the IFE. AA reduced Cr(VI) to Cr(III) and weakened the IFE between Cr(VI) and N,S-CDs, which restored the FL of N,S-CDs. The "on–off–on" FL technique was also successfully used to detect Cr(VI) and AA in real samples. In addition, the CCK-8 assay proved that the N,S-CDs had low toxicity. This work presented a superior fluorescent sensor for quantification of Cr(VI) and AA, and also provided a new idea to transform seaweeds to high value-added products.

Conflicts of interest

There are no conflicts to declare.

Acknowledgements

This work was financially supported by the Key Research and Development Plan of Hainan Province (ZDYF2018232), Hainan

Provincial Natural Science Foundation of China (Grant No. 521QN205), the National College Student Innovation and Entrepreneurship Training Program (202010589083), the Graduate Innovative Research Project of Hainan Province (Hyb2020-22).

Notes and references

1 A. P. Rawat and D. J. Singh, *Ecotoxicol. Environ. Saf.*, 2019, **176**, 27–33.
2 G. Qiao, D. Lu, Y. Tang, J. Gao and Q. Wang, *Dyes Pigm.*, 2019, **163**, 102–110.
3 J. L. Liu, X. R. Xu, Z. H. Ding, J. X. Peng, M. H. Jin, Y. S. Wang, Y. G. Hong and W. Z. Yue, *Ecotoxicology*, 2015, **24**, 1583–1592.
4 T. P. Rao, S. Karthikeyan, B. Vijayalekshmy and C. Iyer, *Anal. Chim. Acta*, 1998, **369**, 69–77.
5 S. A. Miscoria, C. Jacq, T. Maeder and R. Martín Negri, *Sens. Actuators, B*, 2014, **195**, 294–302.
6 S. K. Tammina and Y. Yang, *J. Photochem. Photobiol., A*, 2020, **387**, 112134.
7 X. Luo, W. Zhang, Y. Han, X. Chen, L. Zhu, W. Tang, J. Wang, T. Yue and Z. Li, *Food Chem.*, 2018, **258**, 214–221.
8 J. F. Y. Fong, S. F. Chin and S. M. Ng, *Biosens. Bioelectron.*, 2016, **85**, 844–852.
9 J. Peng, J. Ling, X.-Q. Zhang, L.-Y. Zhang, Q.-E. Cao and Z.-T. Ding, *Sens. Actuators, B*, 2015, **221**, 708–716.
10 K. Liu, P. Yu, Y. Lin, Y. Wang, T. Ohsaka and L. Mao, *Anal. Chem.*, 2013, **85**, 9947–9954.
11 P. Koblová, H. Sklenářová, I. Brabcová and P. Solich, *Anal. Methods*, 2012, **4**, 1588–1591.
12 X. Wu, Y. Diao, C. Sun, J. Yang, Y. Wang and S. Sun, *Talanta*, 2003, **59**, 95–99.
13 Z. Wang, X. Teng and C. Lu, *Analyst*, 2012, **137**, 1876–1881.
14 X. Zhu, T. Zhao, Z. Nie, Y. Liu and S. Yao, *Anal. Chem.*, 2015, **87**, 8524–8530.
15 C. Sun, X. Gao, L. Wang and N. Zhou, *Food Anal. Methods*, 2021, **14**, 1121–1132.
16 S. N. Baker and G. A. Baker, *Angew. Chem., Int. Ed.*, 2010, **49**, 6726–6744.
17 R. Das, R. Bandyopadhyay and P. Pramanik, *Mater. Today Chem.*, 2018, **8**, 96–109.
18 H. Ma, C. Sun, G. Xue, G. Wu, X. Zhang, X. Han, X. Qi, X. Lv, H. Sun and J. Zhang, *Spectrochim. Acta, Part A*, 2019, **213**, 281–287.
19 A. B. Pebdeni, M. Hosseini and M. R. Ganjali, *Food Anal. Methods*, 2020, **13**, 2070–2079.
20 Y. Feng, D. Zhong, H. Miao and X. Yang, *Talanta*, 2015, **140**, 128–133.
21 Z. Qin, K. Xu, H. Yue, H. Wang, J. Zhang, C. Ouyang, C. Xie and D. Zeng, *Sens. Actuators, B*, 2018, **262**, 771–779.
22 A. Yari and H. Bagheri, *J. Chin. Chem. Soc.*, 2009, **56**, 289–295.
23 Z. Song, F. Quan, Y. Xu, M. Liu, L. Cui and J. Liu, *Carbon*, 2016, **104**, 169–178.
24 D. Gu, S. Shang, Q. Yu and J. Shen, *Appl. Surf. Sci.*, 2016, **390**, 38–42.
25 K. Chen, J. J. Ríos, A. Pérez-Gálvez and M. Roca, *Food Chem.*, 2017, **228**, 625–633.
26 L. N. White and W. L. White, *Bot. Mar.*, 2020, **63**, 303–313.
27 I. Novoa-De León, J. Johny, S. Vázquez-Rodríguez, N. García-Gómez, S. Carranza-Bernal, I. Mendivil, S. Shaji and S. Sepúlveda-Guzmán, *Carbon*, 2019, **150**, 455–464.
28 H. Tian, H. Liu, W. Song, L. Zhu, T. Zhang, R. Li and X. Yin, *Algal Res.*, 2020, **49**, 101853.
29 M. Wang, R. Shi, M. Gao, K. Zhang, L. Deng, Q. Fu, L. Wang and D. Gao, *Food Chem.*, 2020, **318**, 126506.
30 C. Xia, S. Zhu, T. Feng, M. Yang and B. Yang, *Adv. Sci.*, 2019, **6**, 1901316.
31 C. J. Jeong, A. K. Roy, S. H. Kim, J.-E. Lee, J. H. Jeong, I. In and S. Y. Park, *Nanoscale*, 2014, **6**, 15196–15202.
32 J. Zhang, W. Shen, D. Pan, Z. Zhang, Y. Fang and M. J. Wu, *New J. Chem.*, 2010, **34**, 591–593.
33 X. Yang, Y. Zhuo, S. Zhu, Y. Luo, Y. Feng and Y. Dou, *Biosens. Bioelectron.*, 2014, **60**, 292–298.
34 W. Yang, J. Ni, F. Luo, W. Weng, Q. Wei, Z. Lin and G. Chen, *Anal. Chem.*, 2017, **89**, 8384–8390.
35 Z. Guo, J. Luo, Z. Zhu, Z. Sun, X. Zhang, Z.-c. Wu, F. Mo and A. Guan, *Dyes Pigm.*, 2020, **173**, 107952.
36 H. Wang, Q. Lu, Y. Hou, Y. Liu and Y. Zhang, *Talanta*, 2016, **155**, 62–69.
37 D. Gu, S. Shang, Q. Yu and J. Shen, *Appl. Surf. Sci.*, 2016, **390**, 38–42.
38 X. Liao, C. Chen, R. Zhou, Q. Huang, Q. Liang, Z. Huang, Y. Zhang, H. Hu and Y. Liang, *Dyes Pigm.*, 2020, **183**, 108725.
39 B. Fang, X. Lu, J. Hu, G. Zhang, X. Zheng, L. He, J. Cao, J. Gu and F. Cao, *J. Colloid Interface Sci.*, 2019, **536**, 516–525.
40 X. Wu, B. Zhao, J. Zhang, H. Xu, K. Xu and G. J. T. Chen, *J. Phys. Chem. C*, 2019, **123**, 25570–25578.
41 Z. Song, F. Quan, Y. Xu, M. Liu, L. Cui and J. Liu, *Carbon*, 2016, **104**, 169–178.
42 K. Chen, W. Qing, W. Hu, M. Lu, Y. Wang and X. Liu, *Spectrochim. Acta, Part A*, 2019, **213**, 228–234.
43 H. Wang, X. Na, S. Liu, H. Liu, L. Zhang, M. Xie, Z. Jiang, F. Han, Y. Li and S. Cheng, *Talanta*, 2019, **201**, 388–396.
44 D. Bu, Y. Wang, N. Wu, W. Feng, D. Wei, Z. Li and M. Yu, *Chin. Chem. Lett.*, 2021, **32**, 1799–1802.
45 Y. Li, Y. Ban, R. Wang, Z. Wang, Z. Li, C. Fang and M. Yu, *Chin. Chem. Lett.*, 2020, **31**, 443–446.
46 G. Hu, L. Ge, Y. Li, M. Mukhtar, B. Shen, D. Yang and J. Li, *J. Colloid Interface Sci.*, 2020, **579**, 96–108.
47 J. Zhang, X. Liu, J. Zhou, X. Huang, D. Xie, J. Ni and C. Ni, *Nanoscale Adv.*, 2019, **1**, 2151–2156.
48 X. Gong, Y. Liu, Z. Yang, S. Shuang, Z. Zhang and C. Dong, *Anal. Chim. Acta*, 2017, **968**, 85–96.
49 M. Cao, Y. Li, Y. Zhao, C. Shen, H. Zhang and Y. Huang, *RSC Adv.*, 2019, **9**, 8230–8238.
50 A. Tall, F. Antônio Cunha, B. Kaboré, C. A. E. S. Barbosa, U. Rocha, T. O. Sales, M. O. Fonseca Goulart, I. Tapsoba and J. Carinhanha Caldas Santos, *Microchem. J.*, 2021, **166**, 106219.
51 D. Das and R. K. Dutta, *ACS Appl. Nano Mater.*, 2021, **4**, 3444–3454.
52 Z. Ramezani, M. Qorbanpour and N. Rahbar, *Colloids Surf., A*, 2018, **549**, 58–66.